Shank3a/b isoforms regulate the susceptibility to seizures and thalamocortical development in the early postnatal period of mice

奥園, 清香

Neuroscience Research 193 (2023) 13–19

Contents lists available at ScienceDirect

Neuroscience Research

journal homepage: www.sciencedirect.com/journal/neuroscience-research

Shank3a/b isoforms regulate the susceptibility to seizures and thalamocortical development in the early postnatal period of mice

Sayaka Okuzono [a,b], Fumihiko Fujii [a], Yuki Matsushita [a], Daiki Setoyama [c], Yohei Shinmyo [d], Ryoji Taira [a], Kousuke Yonemoto [a], Satoshi Akamine [a], Yoshitomo Motomura [a], Masafumi Sanefuji [a], Takeshi Sakurai [e], Hiroshi Kawasaki [d], Kihoon Han [f], Takahiro A. Kato [g], Hiroyuki Torisu [b], Dongchon Kang [c], Yusaku Nakabeppu [h], Yasunari Sakai [a,*,1], Shouichi Ohga [a]

[a] Department of Pediatrics, Graduate School of Medical Sciences, Kyushu University, Fukuoka 812-8582, Japan
[b] Section of Pediatrics, Department of Medicine, Fukuoka Dental College, Fukuoka 814-0193, Japan
[c] Department of Clinical Chemistry and Laboratory Medicine, Graduate School of Medical Sciences, Kyushu University, Fukuoka 812-8582, Japan
[d] Department of Medical Neuroscience, Graduate School of Medical Sciences, Kanazawa University, Kanazawa 920-8640, Japan
[e] Medical Innovation Center, Kyoto University Graduate School of Medicine, Kyoto 606-8507, Japan
[f] Department of Neuroscience, Korea University College of Medicine, Seoul 02841, Republic of Korea
[g] Department of Neuropsychiatry, Graduate School of Medical Sciences, Kyushu University, Fukuoka 812-8582, Japan
[h] Division of Neurofunctional Genomics, Medical Institute of Bioregulation, Kyushu University, Fukuoka 812-8582, Japan

ARTICLE INFO

Keywords:
Autism spectrum disorder (ASD)
SH3 and ankyrin-repeat domain containing 3 (SHANK3)
Thalamus
Seizures

ABSTRACT

Epileptic seizures are distinct but frequent comorbidities in children with autism spectrum disorder (ASD). The hyperexcitability of cortical and subcortical neurons appears to be involved in both phenotypes. However, little information is available concerning which genes are involved and how they regulate the excitability of the thalamocortical network. In this study, we investigate whether an ASD-associated gene, *SH3 and multiple ankyrin repeat domains 3* (*Shank3*), plays a unique role in the postnatal development of thalamocortical neurons. We herein report that Shank3a/b, the splicing isoforms of mouse Shank3, were uniquely expressed in the thalamic nuclei, peaking from two to four weeks after birth. Shank3a/b-knockout mice showed lower parvalbumin signals in the thalamic nuclei. Consistently, Shank3a/b-knockout mice were more susceptible to generalized seizures than wild-type mice after kainic acid treatments. Together, these data indicate that NT-Ank domain of Shank3a/b regulates molecular pathways that protect thalamocortical neurons from hyperexcitability during the early postnatal period of mice.

1. Introduction

Autism spectrum disorder (ASD) is an increasingly recognized group of neurodevelopmental diseases characterized by restricted interests and deficits in social skills (Sasayama et al., 2021). Ten to 20% of children with ASD develop epileptic seizures that need medication (Liu et al., 2021). The high comorbidity rate of epilepsy with ASD suggests common mechanisms underlying the two phenotypes (Lee et al., 2015).

Epileptic seizures in patients with ASD are typically characterized as a tonic-clonic pattern or as a focal-onset, secondarily generalized forms (Jeste and Tuchman, 2015). The nosology suggests that seizures in ASD involve thalamic neurons and dysfunctions of gamma aminobutyric acid (GABA)-producing interneurons in thalamocortical circuits (Caciagli et al., 2020). Little is known, however, about which genes are involved or how they regulate the postnatal development of thalamic interneurons and thalamocortical connectivity.

Among the genes located at 22q13.3, the deletion of *SH3 and multiple ankyrin repeat domains 3* (*SHANK3*) is critical for the neurodevelopmental phenotypes of Phelan-McDermid syndrome (PMS) (Monteiro and Feng, 2017). Because *SHANK3* plays an essential role in the synaptic development (Monteiro and Feng, 2017; Naisbitt et al., 1999), dissecting the molecular functions of *SHANK3* in the developing brain provides a clue to understand the pathogenic mechanisms of neurobehavioral problems in affected children (Monteiro and Feng,

* Correspondence to: Department of Pediatrics, Graduate School of Medical Sciences, Kyushu University, 3-1-1 Maidashi, Higashi-ku, Fukuoka 812-8582, Japan.
E-mail address: sakai.yasunari.530@m.kyushu-u.ac.jp (Y. Sakai).
[1] ORCiD: https://orcid.org/0000-0002-5747-8692

https://doi.org/10.1016/j.neures.2023.03.001
Received 19 December 2022; Received in revised form 19 February 2023; Accepted 1 March 2023
Available online 5 March 2023

2017). Notably, the mouse brain expresses multiple isoforms of Shank3 (Shank3a-f) via alternative splicing (Wang et al., 2014), although their distinct roles remain to be defined.

The two isoforms of murine Shank3 containing the ankyrin repeat domain (Ank) are designated Shank3a/b (Bucher et al., 2021; Cai et al., 2020, 2021; Monteiro and Feng, 2017; Sakai et al., 2022; Salomaa et al., 2021). In the present study, we investigated whether or not the Shank3a/b isoforms play indispensable roles in the development of the thalamic function in the early postnatal life of humans and mice. We found that Shank3a/b was highly expressed in the thalamic nuclei of mice at two to four weeks old. In agreement with this finding, Shank3a/b-knockout (KO) mice showed lower parvalbumin (Pvalb) signals in the thalamic nuclei than wild-type mice and greater susceptibility to kainic acid-induced seizures. Our data thus indicate that Shank3a/b plays an essential role in organizing the excitation-inhibition (EI) balance of thalamocortical circuits during the early postnatal period.

2. Materials and methods

2.1. Ethics

Animal experiments were performed in accordance with the ARRIVE guidelines. Specific protocols and were approved by the Institutional Animal Care and Use Committee (#A21–422–0 and A21–189–1), which is associated with the National Research Council's Guide for the Care and Use of Laboratory Animals.

2.2. Animals

Shank3$^{tm1a(KOMP)Wtsi}$ mice were purchased from KOMP (Bozdagi et al., 2010). Mice were maintained in a specific-pathogen-free environment. Tissue sampling was conducted under deep anesthesia with inhalation of sevoflurane. Four-week-old male WT, Shank3a/b-KO and heterozygous littermates were subjected to quantitative PCR, Western blotting and immunofluorescence studies unless otherwise stated.

2.3. Quantitative PCR

The relative gene expression was calculated by the ddCt method (Akamine et al., 2020). Mouse *Actb* was used as an internal control. PCR primers used in this study are listed in Table S1.

2.4. Kainic acid treatment

Four-week-old male littermates were used for this study. Mice were injected intraperitoneally with either saline (vehicle) or kainic acid (KA) (Wako, Osaka, Japan) dissolved in saline. KA was administered at a dose of 10 mg/kg for the experiment. To assess the onset and severity of seizures, we recorded the seizure score for 1 hr after KA treatments using the standard scale: 0, no reaction; 1, arrest of motion; 2, myoclonic jerks of the head and neck, with brief twitching movements; 3, unilateral clonic activity; 4, bilateral forelimb tonic and clonic activity; and 5, generalized tonic-clonic activity with loss of postural tone including death from continuous convulsion, according to the previously described criteria (Yang et al., 1997).

2.5. Immunofluorescence

Standard methods were used as previously described (Akamine et al., 2020; Matsushita et al., 2016). Antibodies are listed in Table 1. Confocal images were obtained with A1 HD25 (Nikon Corporation, Tokyo, Japan). Image processing and digital stitching were performed with the NIS-elements AR software program (Nikon Corporation). BZ-X800 (Keyence, Osaka, Japan) equipped with the analytical software program BZ-X analyzer (Keyence) was used for the quantitative analysis.

Table 1
Antibodies used in this study.

Item	Catalog #	Vendor[1]	Experiment[2]	Dilution
anti-β-actin	ab49900	Ab	WB	1:50,000
anti-β-galactosidase	ab9361	Ab	IF	1:1000
anti-Calbindin	ab108404	Abcam	WB	1:1000
anti-Gad67	MAB5406	SA	IF	1:1000
anti-Homer	sc-15321	SCB	WB	1:1000
anti-Pvalb	MAB1572	SA	IF	1:1000
anti-Shank1 [N22/21]	ab94576	Ab	IF	1:100
anti-Shank2 [B-4]	sc-365121	SCB	IF	1:100
anti-Shank3 [C-4]	sc-377088	SCB	IF	1:100
			WB	1:1000
anti-Shank3 [H-160]	sc-30193	SCB	IF	1:100

Ab, Abcam; SA, Sigma-Aldrich; SCB, Santa Cruz Biotechnology
IF, immunofluorescence; WB, Western blotting

The ImageJ software program (https://imagej.nih.gov/ij/) was used for the quantitative measurement of fluorescence signals.

2.6. Western blotting

Standard methods were used (Akamine et al., 2020; Matsushita et al., 2016). A 4–15% polyacrylamide electrophoresis gel (Mini-PROTEAN TGX Gels; BioRad Laboratories, Hercules, CA, USA) was loaded with 20–50 μg protein per lane. Ponceau S staining (A40000279; Thermo Fisher Scientific) was used for testing the condition of electro-transfer. Antibodies are listed in Table 1.

2.7. Statistical analysis

All statistical analyses were performed using R (https://cran.r-project.org/) and the JMP software program (SAS Institute, Cary, NC, USA). The collected data are presented as the mean ± standard deviation (SDM) unless otherwise stated. P values of < 0.05 (*) were considered significant ($^{**}p < 0.01$; and $^{***}p < 0.001$).

3. Results

3.1. Expression of Shank3 isoforms in the postnatal brain

To investigate whether Shank3a plays a distinct role from other isoforms in the developing brain, we used *Shank3*$^{flox\ ex4–9/flox\ ex4–9}$ mice (Fig. 1**A**) (Bozdagi et al., 2010). The *Shank3*$^{flox\ ex4–9}$ (knockout, KO) allele disrupted the expression of Shank3a (180 kDa) while it allowed the downstream promoters and alternative exons to express the smaller (c-f) isoforms (118–150 kDa, Fig. 1**B, C**). We used the mouse monoclonal anti-Shank3 antibody (C-4), which detects the amino acid 1431–1590, a conserved region among Shank3a-f isoforms (Fig. 1**B**). We ensured that Shank3a/b-KO mice, but not the wild-type (WT) mice, expressed β-galactosidase (β-Gal) in the postnatal brain at 4 weeks of age (Fig. 1**D**). Because the presence of β-Gal signals reflected tissues that lacked the endogenous expression of Shank3a/b, the immunofluorescence data suggested that Shank3a/b was strongly expressed in the thalamus, cerebral cortex and hippocampus (Fig. 1**E**).

To further validate this finding, we evaluated the expression of *Shank3a/b* mRNA containing exons 7–9. WT and heterozygous mice expressed, but not Shank3a/b-KO mice did, *Shank3a/b* mRNA in cerebral cortices, hippocampi and thalami (Fig. S1**,** upper). In contrast, common splicing isoforms spanning exons 12 and 13 were present at similar levels in these tissues from WT, heterozygous and Shank3a/b-KO mice (Fig. S1, middle). Cerebral cortices, hippocampi and thalami from heterozygous and Shank3a/b-KO mice showed $\geq$1000-fold *lacZ* expression compared with WT mice (Fig. S1, lower). Thus, the *lacZ* mRNA expression was inversely correlated with the Shank3a/b expression, and β-Gal signals indicated the specific brain regions where WT mice expressed the Shank3a/b isoforms.

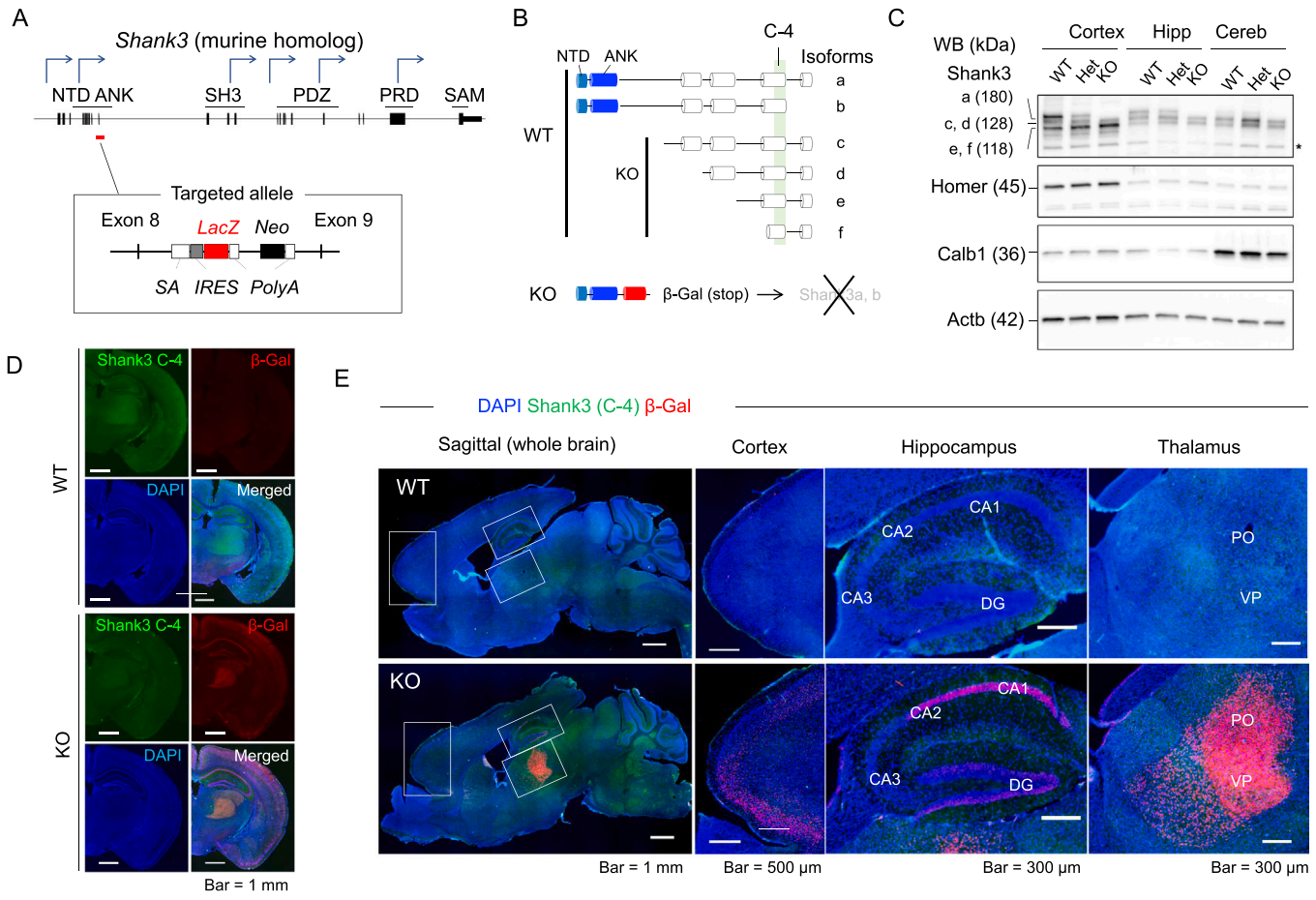

Fig. 1. The expression pattern of Shank3 isoforms. A schematic view of the mouse *Shank3* gene. Arrows indicate the transcriptional initiation sites. The targeted allele has stop codon and *lacZ* sequence (red) between exons 8 and 9. Shank3a/b are translated from the WT mRNA, but not from the KO mRNA. NTD-Ank (blue columns) and other domains (white) are depicted. The KO allele expresses β-Gal. Green shade represents the epitope region of anti-Shank3, C-4. Western blotting for WT, heterozygous (het) and Shank3a/b-KO brain extracts. Homer1 and calbindin are tissue markers for the cerebellum and cortex, respectively. (D, E) Coronal (D) and sagittal (E) views of WT and Shank3a/b-KO mouse brain at 4 weeks of age. Anti-β-Gal (red) and Shank3 (green, mouse clone #C-4) were used. β-Gal signals are present in the cerebral cortex, hippocampus and thalamus of KO mice.

We ensured that all three Shank family proteins appeared to be ubiquitously expressed in the cerebral cortex, hippocampus and thalamus at this age (Fig. S2A, **B**). However, only the mouse monoclonal anti-Shank3 (#C-4) antibody, but not the rabbit polyclonal anti-Shank3, detected regionally hyperintense signals of Shank3 in the thalamic nuclei (Fig. S3A, **B**). In contrast to WT mice, the laminar-gradient pattern of Shank3 signals was hardly observed in the cerebral cortex of Shank3a/b-heterozygous or KO mice (Fig. S4A, **B**). Shank3a/b-heterozygous or KO mice did not show hyperintense signals of Shank3 in the thalamic nuclei, either (Fig. S4A, **B**). Regionally hyperintense signals of Shank3 were likely to reflect the biallelic expression of Shank3a/b in the thalamus at 4 weeks of age. Anti-Shank3 (#C-4) also detected the ubiquitously expressed signals of Shank3c-f isoforms, harboring the common epitope of PDZ, rather than the cross-reacting signals of the antibody with Shank1 and Shank2.

We further ensured that the mouse monoclonal anti-Shank3 (C-4) clearly detected the 180-kD band of Shank3a in comparison with rabbit anti-Shank3a in Western blotting (Fig. S5). Thus, both in Western blotting (Fig. 1**C, S5**) and immunofluorescence (Figs. 1**D, E and** 2**A**) studies, the antibody C-4 clarified the unique expression of Shank3a/b in the WT mouse brain.

3.2. *Expression of Shank3a/b in the postnatal brain*

To clarify the expression of Shank3a/b at an early postnatal age, we assessed the time course of β-Gal expression in heterozygous mice from 1 to 16 weeks. The thalamic β-Gal signal was highest at two weeks of age and then gradually decreased with age ($p = 5.3 \times 10^{-6}$, two-way ANOVA; Fig. 2**A, B**). The expression of Shank3 isoforms containing the common epitope was gradually increased during this period (Fig. 2**A, B**). In qPCR, the expression of Shank3a/b-encoding mRNA (exons 7–9) was elevated from 2 to 4 weeks after birth, whereas the expression of mRNA harboring common exons (exons 12–13) increased during the observation period (1–8 weeks of age) ($p = 0.028$, two-way ANOVA; Fig. 2**C**). Western blotting also showed that the expression of Shank3a (180 kDa) was gradually declined during postnatal weeks 2–8 in the cerebral cortex of WT mice (Fig. 2**D**, left). In contrast, the higher expression ratio (Shank3a/e) was observed in the thalamus than in the cerebral cortex during that same period (Fig. 2**D**, right). Thus, the expression of Shank3a/b was differentially regulated from those of other isoforms in each brain region.

3.3. *Decreased parvalbumin signals in Shank3a/b-KO mice*

Loss of *Shank3* was reported to cause decrease in the expression of parvalbumin (Pvalb), but not the number of Pvalb+ neurons (Filice et al., 2016). Because Shank3a/b was highly expressed in thalamic nuclei (Fig. 1**D, E**), we rationalized that similar findings might be observed in this region with Shank3a/b-KO mice. Shank3a/b-KO mice showed lower Pvalb+ signals in the thalamic ventral posteromedial

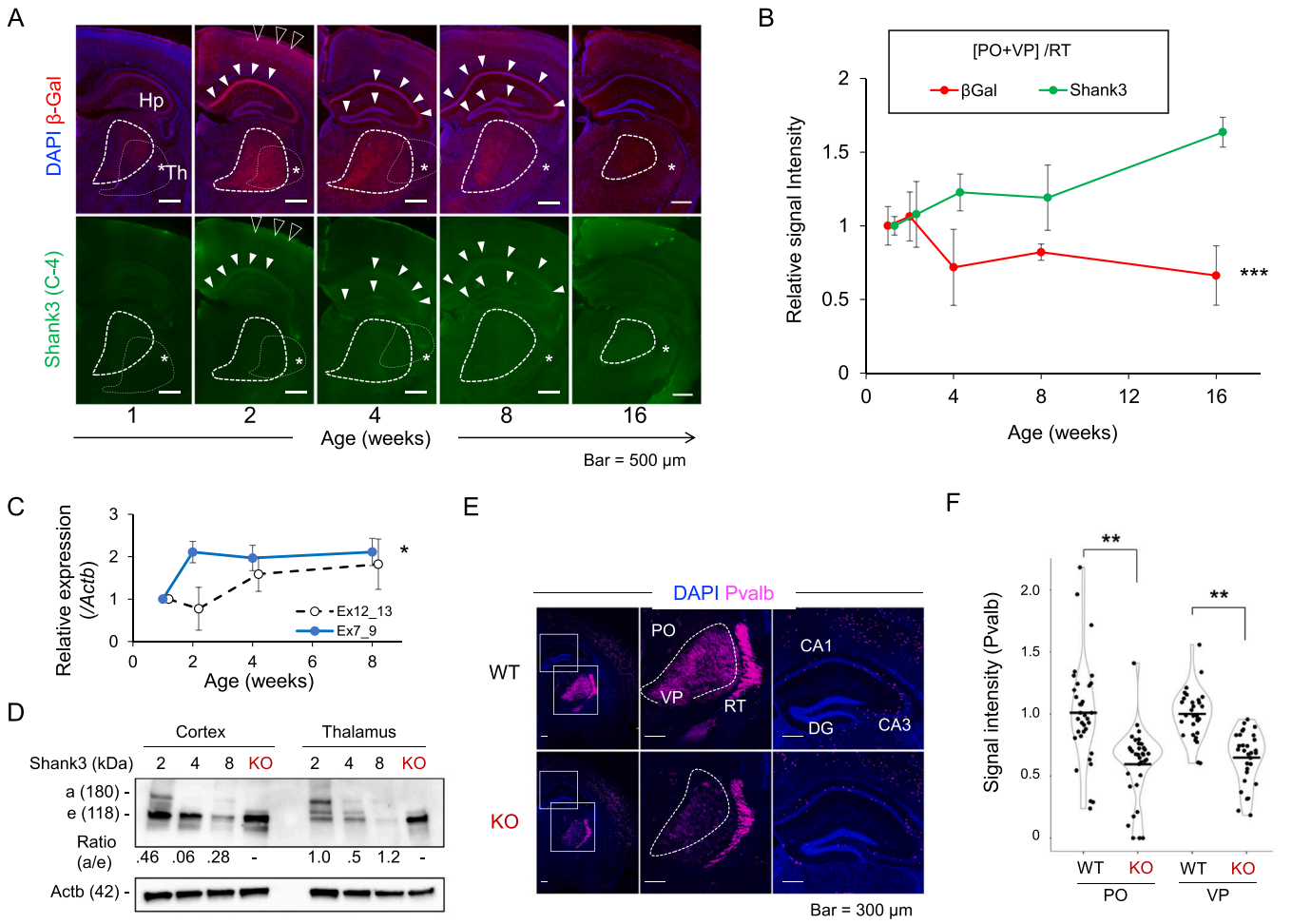

Fig. 2. Shank3a/b expression during the postnatal period. Expression of β-Gal (red) and Shank3 (#C-4, green) at different ages. A serial immunofluorescence using the brains from heterozygous male mice. Dashed circles indicate PO+VPM. Arrowheads, high-intensity signals of Shank3 and their corresponding signals to β-Gal (lucent = cortex, white = hippocampus; Asterisks, reference regions (thalamic RT) for the quantitative measurement of Shank3 signals). Quantitative measurements of data in (A). Line plots show β-Gal and Shank3 signals per PO+VPM area (mean ± SDM, n = 3–7 at each age; reference: 2 weeks of age). Relative expression of mRNA containing Shank3a/b-specific exons 7–9 (blue) and common exons 12–13 (white). The qPCR data show data using the thalamus from WT mice (mean ± SDM, n = 3 for each time point). Expression of Shank3a/b and c-e protein isoforms in the cerebral cortex and thalamus at the indicated age of WT mice. Ratio (a/e) represents the relative signal intensity of Shank3a to Shank3e at the indicated age of WT mice. -, uncalculated. Western blotting with 50 μg total protein/lane. Coronal sections of WT and Shank3a/b-KO thalami at 4 weeks of age. Note, Pvalb (magenta) signals in ventroposterior (VP) and posterior (PO) thalamic nuclei in KO mice are decreased. Sections are stained with DAPI and anti-Pvalb antibody. A quantitative analysis for immunofluorescence of Pvalb in panel E. (E; n = 20 from 3 pairs of littermates). Each dot represents the signal intensity of Pvalb in an area-adjusted region of interest (10 areas in VP and PO from 1 section). Reticular nucleus (RT), reference region.

(VPM), posterior thalamic nuclei (PO) nuclei and hippocampal CA1 than WT mice at 4 weeks of age ($p < 0.001$, <0.001 and 0.028 respectively; Wilcoxon's rank sum tests; Fig. 2**E, F** and **S6A**). Pvalb signals did not differ in the hippocampal the CA2, CA3 or dentate gyrus (DG) between the two mouse strains (Fig. S6B). Immunofluorescence signals of other GABAergic interneuron markers (Gad67) did not differ between Shank3a/b-KO and WT mice in VPM neurons (Fig. S6C). In PO neurons, higher signals of Gad were observed in WT than in KO mice ($p = 0.0108$).

3.4. *Exaggeration of kainic acid-induced seizures in Shank3a/b-KO mice*

Reduced Pvalb signals in Shank3a/b-KO mice suggested that they might show higher susceptibility to seizures than WT mice. To examine this, we employed a seizure model using KA, a potent inducer of focal and generalized seizures in mice (Kajitani et al., 2006). During the whole observation period (0–60 min), the seizure scores of Shank3a/b-KO mice were significantly higher than those of WT mice ($p < 2.2 \times 10^{-16}$; repeated two-way ANOVA [time, genotype]; Fig. 3**A**). The heterozygous mice were also as susceptible to KA-induced seizures as Shank3a/b-KO mice ($p = 4.1 \times 10^{-14}$; repeated two-way ANOVA; Fig. 3**A**), indicating the haploinsufficiency of *Shank3a/b* deletion. During the early phase, severe seizures (grade 3–5) were never observed in either WT, heterozygous or Shank3a/b-KO mice (Fig. 3**B**, 0–10 min). However, both Shank3a/b-heterozygous and KO mice developed severe seizures more frequently (29–51%) than WT mice (0–7.8%) during the late phase ($p < 0.001$, Tukey' HSD; Fig. 3**B**, 50–60 min).

4. Discussion

This study first clarified that the expression of the NT-Ank-containing isoform Shank3a/b was temporally and spatially regulated during the postnatal period in mice. Knowing that Shank3a/b was highly expressed in the thalamic nuclei, we hypothesized that this isoform might play an important role in the development of neural circuits in the early postnatal stage.

Clinically, 27–70% of patients with PMS develop epilepsy (Holder and Quach, 2016). Of note, atypical absence seizure has been reported to

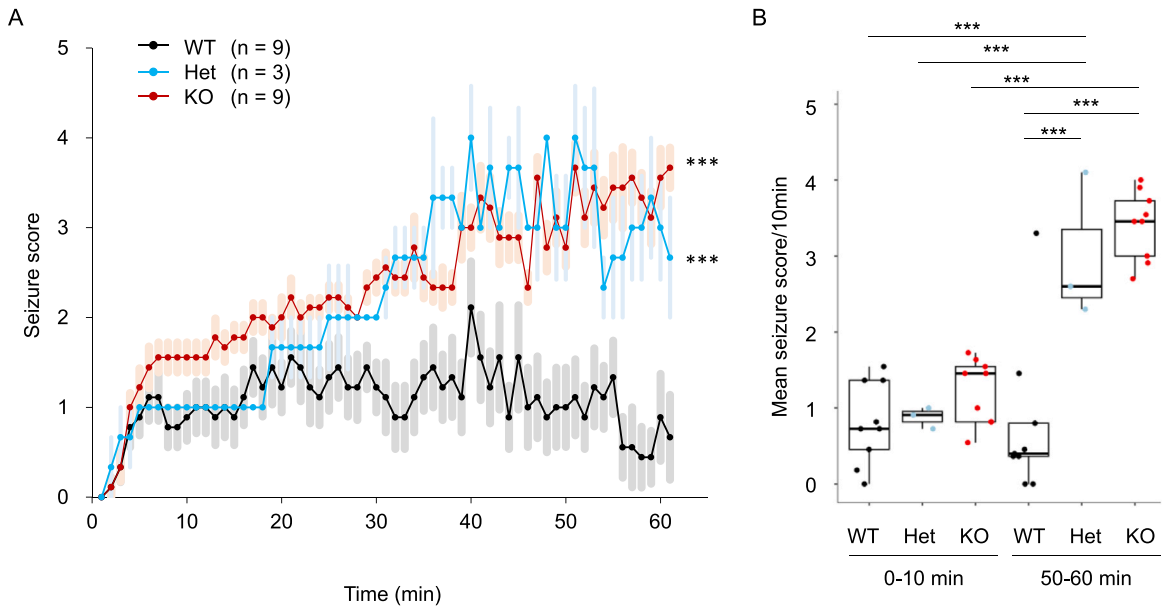

Fig. 3. Susceptibility of Shank3a/b-knockout mice to kainic acid-induced seizures. A.Time course of seizures (mean ± SEM values) after kainic acid (KA) injection for 4-week-old WT (black), Shank3a/b-KO (red) and heterozygous (blue) male mice. B.The average score of seizure events in the early phase (0–10 min, left) and the late phase (50–60 min, right) after KA treatment.

be the most prevalent form of epilepsy in patients with *SHANK3* mutations and PMS (Holder and Quach, 2016). Furthermore, 2 (8%) of 24 patients with PMS developed Lennox-Gastaut syndrome, the most severe form of epileptic encephalopathy in childhood (Holder and Quach, 2016). Because both absence seizure and Lennox-Gastaut syndrome involve thalamocortical dysfunction as an epileptogenic mechanism (Warren et al., 2017), susceptibility to seizures in patients with PMS may involve an increased excitability of thalamus and thalamocortical circuits.

Several mouse lines have been established to disrupt or attenuate the physiological functions of Pvalb interneurons in the thalamic reticular nucleus (Abdelaal et al., 2022; Calin et al., 2021; Godoy et al., 2022; Leitch, 2022; Makinson et al., 2017; Panthi and Leitch, 2019). Dysfunction of thalamic Pvalb interneurons caused mice to develop spike-and-wave discharges and absence-like seizures. Of note, functional disruption of AMPA receptor subunit GluA4 led to selective impairment in feed-forward inhibition at corticothalamic (CT)-reticular thalamic nucleus (RTN) synapses, which underlies the epileptogenic discharges and absence seizure in mice (Leitch, 2022). Furthermore, hypo-functioning of mTORC1 and 4E-BP2-dependent translation in Pvalb interneurons critically increased susceptibility to both pentylenetetrazole (PTZ)- and kainic acid (KA)-induced seizures (Sharma et al., 2021). In contrast, activation of Pvalb interneurons using an optogenetic system showed a suppressive effect on cortical and thalamic seizures (Chang et al., 2017). Thus, the reduced expression of Pvalb in the thalamic nuclei reasonably explained the epileptogenic phenotype of Shank3a/b-KO mice in this study.

From a biochemical perspective, an increasing number of molecules have been reported to interact with the NT-Ank domain of Shank3. NT-Ank regulates multiple molecular pathways associated with cytoskeletal remodeling (F-actin, α-spectrin) (Bockers et al., 2001; Durand et al., 2012; Han et al., 2013; Salomaa et al., 2021), β- and δ-catenin (Hassani Nia et al., 2020a, 2020b; Schmeisser et al., 2009) and Ras and Rap1 GTP-binding proteins (Lilja et al., 2017; Salomaa et al., 2021). Our data suggested that these interactions may exert unique effects on the development of thalamocortical circuits in the postnatal period of mice and humans.

In humans, little information is available concerning the region-specific expression of SHANK3a-f isoforms (Maunakea et al., 2010). A molecular study showed that five CpG islands (CGI-1 to CGI-5) in SHANK3 were uniquely methylated in different brain regions (cerebellum vs. Broadman's area 19) (Zhu et al., 2014). The postmortem brain from ASD patients showed hypermethylated conditions of SHANK3 (CGI-2, 3 and 4), which resulted in the lower expression of SHANK3c and e isoforms in the cerebellum than controls. Those authors further found that the increased methylation of CGI-2 and CGI-4 was associated with the reduced expression of SHANK3c in brain tissues and reduced promoter activity in cultured cells. These data suggested that the expression of human SHANK3 is epigenetically regulated through a complex mechanism. Thus far, however, no epigenetic studies have linked the intragenic methylation of SHANK3 (CGI-1) with the region-specific or age-dependent expression of SHANK3a/b isoforms, particularly in childhood. Given the high comorbidity rates of epilepsy and somatosensory disturbance in children with PMS, our study might provide insight into the functional role of SHANK3a/b in the postnatal development of the human brain.

Dysfunction of Pvalb interneurons is also associated with neurodevelopmental and psychiatric conditions in multiple mouse models (Ruden et al., 2021). For example, knockout of the gene responsible for Rett syndrome, methyl CpG binding protein 2 (Mecp2), shows repetitive behaviors and stereotypies even if the gene is selectively removed from Pvalb interneurons (Ito-Ishida et al., 2015). Reduced numbers and/or immunoreactivity of Pvalb interneurons were reproducibly observed in mice with deletion of contactin associated protein 2 (Cntnap2) (Lauber et al., 2018; Penagarikano et al., 2011; Selimbeyoglu et al., 2017), conditional knockout of all three neurexins (Chen et al., 2017), and in Shank models (Filice et al., 2016; Lee et al., 2018; Mao et al., 2015). Unlike Shank3a/b-KO mice, however, conditional deletion of Shank2 in Pvalb interneurons did not augment seizure susceptibility or paroxysmal discharges in electroencephalography although they showed hyperactivity and enhanced self-grooming behaviors (Lee et al., 2018). Nonetheless, these studies postulated the concept that pathogenic mechanisms of neurodevelopmental and psychiatric diseases may converge at hypo-functioning Pvalb interneurons in mice and humans (Gandal et al., 2018, 2022). Thus, it is worth clarifying the specific roles of thalamic Pvalb interneurons during the early postnatal period.

Several limitations remain in the present study. Video-monitoring electroencephalograms may detect nonconvulsive epileptic seizures,

such as absence seizure, in addition to KA-induced seizures. We also need to test whether the striatal expression of Shank3 also plays a major role in the postnatal development of thalamocortical circuits (Peca et al., 2011). Single-cell RNA sequencing for conditional *Shank3a/*b-knockout mice will clarify which neurons show aberrant molecular signaling and alternative splicing.

In conclusion, we found that Shank3a/b, the NT-Ank containing isoforms of Shank3, were uniquely expressed in the thalamic nuclei during the early postnatal period. The developmental process of somatosensory and other thalamocortical circuits is a valuable target for identifying the neural bases of ASD.

Author contributions

Okuzono performed the majority of experiments; F.F., Y.M., D.S, Shinmyo, R.T., K.Y. and S.A. supported and supervised the experiments; Y.M., M.S., H.K., T.A.K., H.T., D.K., Y.N. analyzed the data; T.S. and K.H. managed the mouse colonies and supervised bioinformatics; Y.S and Ohga conceptualized this study; Okuzono and Y.S. drafted the manuscript; all authors critically read and approved the contents of this manuscript.

Conflict of interest

The authors declare no competing interests.

Data Availability

Data will be made available on request.

Acknowledgments

We thank Professor Toshiro Hara (President, Fukuoka Children's Hospital), Professor Shigenobu Kanba (Kyushu University), Professor Kazuaki Nonaka (Kyushu University); Ms. Setsuko Kitamura (deceased) for assisting cryo-sectioning; Drs. Koshiro Tagawa, J. Kishimoto and advisors in Center for Clinical and Translational Research (CCTR), Kyushu University Hospital for statistical analysis; and Dr. Tamami Tanaka, Ms. Ayumi Tahara and Ms. Ryoko Unose for assisting with animal experiments. This study was supported by JSPS KAKENHI grant numbers JP21K07865 (Okuzono), JP19K08281 (Sakai); AMED under the grant number JP20ek0109411, JP20wm0325002h; research grants from the Ministry of Health, Labour and Welfare of Japan (JP20FC1054 and JP21FC1005); The Japan Epilepsy Research Foundation, and Kawano Masanori Memorial Public Interest Incorporated Foundation for Promotion of Pediatrics (Sakai).

Appendix A. Supporting information

Supplementary data associated with this article can be found in the online version at doi:10.1016/j.neures.2023.03.001.

References

Abdelaal, M.S., Midorikawa, M., Suzuki, T., Kobayashi, K., Takata, N., Miyata, M., Mimura, M., Tanaka, K.F., 2022. Dysfunction of parvalbumin-expressing cells in the thalamic reticular nucleus induces cortical spike-and-wave discharges and an unconscious state. Brain Commun. 4, fcac010.

Akamine, S., Okuzono, S., Yamamoto, H., Setoyama, D., Sagata, N., Ohgidani, M., Kato, T.A., Ishitani, T., Kato, H., Masuda, K., Matsushita, Y., Ono, H., Ishizaki, Y., Sanefuji, M., Saitsu, H., Matsumoto, N., Kang, D., Kanba, S., Nakabeppu, Y., Sakai, Y., Ohga, S., 2020. GNAO1 organizes the cytoskeletal remodeling and firing of developing neurons. FASEB J. 34, 16601–16621.

Bockers, T.M., Mameza, M.G., Kreutz, M.R., Bockmann, J., Weise, C., Buck, F., Richter, D., Gundelfinger, E.D., Kreienkamp, H.J., 2001. Synaptic scaffolding proteins in rat brain. Ankyrin repeats of the multidomain Shank protein family interact with the cytoskeletal protein alpha-fodrin. J. Biol. Chem. 276, 40104–40112.

Bozdagi, O., Sakurai, T., Papapetrou, D., Wang, X., Dickstein, D.L., Takahashi, N., Kajiwara, Y., Yang, M., Katz, A.M., Scattoni, M.L., Harris, M.J., Saxena, R., Silverman, J.L., Crawley, J.N., Zhou, Q., Hof, P.R., Buxbaum, J.D., 2010. Haploinsufficiency of the autism-associated Shank3 gene leads to deficits in synaptic function, social interaction, and social communication. Mol. Autism 1, 15.

Bucher, M., Niebling, S., Han, Y., Molodenskiy, D., Hassani Nia, F., Kreienkamp, H.J., Svergun, D., Kim, E., Kostyukova, A.S., Kreutz, M.R., Mikhaylova, M., 2021. Autism-associated SHANK3 missense point mutations impact conformational fluctuations and protein turnover at synapses. Elife 10.

Caciagli, L., Allen, L.A., He, X., Trimmel, K., Vos, S.B., Centeno, M., Galovic, M., Sidhu, M.K., Thompson, P.J., Bassett, D.S., Winston, G.P., Duncan, J.S., Koepp, M.J., Sperling, M.R., 2020. Thalamus and focal to bilateral seizures: a multiscale cognitive imaging study. Neurology 95, e2427–e2441.

Cai, Q., Hosokawa, T., Zeng, M., Hayashi, Y., Zhang, M., 2020. Shank3 binds to and stabilizes the active form of Rap1 and HRas GTPases via Its NTD-ANK tandem with distinct mechanisms. Structure 28 (290–300), e294.

Cai, Q., Zeng, M., Wu, X., Wu, H., Zhan, Y., Tian, R., Zhang, M., 2021. CaMKIIalpha-driven, phosphatase-checked postsynaptic plasticity via phase separation. Cell Res. 31, 37–51.

Calin, A., Ilie, A.S., Akerman, C.J., 2021. Disrupting epileptiform activity by preventing parvalbumin interneuron depolarization block. J. Neurosci. 41, 9452–9465.

Chang, W.J., Chang, W.P., Shyu, B.C., 2017. Suppression of cortical seizures by optic stimulation of the reticular thalamus in PV-mhChR2-YFP BAC transgenic mice. Mol. Brain 10, 42.

Chen, L.Y., Jiang, M., Zhang, B., Gokce, O., Sudhof, T.C., 2017. Conditional deletion of all neurexins defines diversity of essential synaptic organizer functions for neurexins. Neuron 94 (611–625), e614.

Durand, C.M., Perroy, J., Loll, F., Perrais, D., Fagni, L., Bourgeron, T., Montcouquiol, M., Sans, N., 2012. SHANK3 mutations identified in autism lead to modification of dendritic spine morphology via an actin-dependent mechanism. Mol. Psychiatry 17, 71–84.

Filice, F., Vorckel, K.J., Sungur, A.O., Wohr, M., Schwaller, B., 2016. Reduction in parvalbumin expression not loss of the parvalbumin-expressing GABA interneuron subpopulation in genetic parvalbumin and shank mouse models of autism. Mol. Brain 9, 10.

Gandal, M.J., Haney, J.R., Parikshak, N.N., Leppa, V., Ramaswami, G., Hartl, C., Schork, A.J., Appadurai, V., Buil, A., Werge, T.M., Liu, C., White, K.P., CommonMind, C., Psych, E.C., i, P.-B.W.G., Horvath, S., Geschwind, D.H., 2018. Shared molecular neuropathology across major psychiatric disorders parallels polygenic overlap. Science 359, 693–697.

Gandal, M.J., Haney, J.R., Wamsley, B., Yap, C.X., Parhami, S., Emani, P.S., Chang, N., Chen, G.T., Hoftman, G.D., de Alba, D., Ramaswami, G., Hartl, C.L., Bhattacharya, A., Luo, C., Jin, T., Wang, D., Kawaguchi, R., Quintero, D., Ou, J., Wu, Y.E., Parikshak, N.N., Swarup, V., Belgard, T.G., Gerstein, M., Pasaniuc, B., Geschwind, D.H., 2022. Broad transcriptomic dysregulation occurs across the cerebral cortex in ASD. Nature.

Godoy, L.D., Prizon, T., Rossignoli, M.T., Leite, J.P., Liberato, J.L., 2022. Parvalbumin role in epilepsy and psychiatric comorbidities: from mechanism to intervention. Front. Integr. Neurosci. 16, 765324.

Han, K., Holder Jr., J.L., Schaaf, C.P., Lu, H., Chen, H., Kang, H., Tang, J., Wu, Z., Hao, S., Cheung, S.W., Yu, P., Sun, H., Breman, A.M., Patel, A., Lu, H.C., Zoghbi, H.Y., 2013. SHANK3 overexpression causes manic-like behaviour with unique pharmacogenetic properties. Nature 503, 72–77.

Hassani Nia, F., Woike, D., Kloth, K., Kortum, F., Kreienkamp, H.J., 2020a. Truncating mutations in SHANK3 associated with global developmental delay interfere with nuclear beta-catenin signaling. J. Neurochem. 155, 250–263.

Hassani Nia, F., Woike, D., Martens, V., Klussendorf, M., Honck, H.H., Harder, S., Kreienkamp, H.J., 2020b. Targeting of delta-catenin to postsynaptic sites through interaction with the Shank3 N-terminus. Mol. Autism 11, 85.

Holder Jr., J.L., Quach, M.M., 2016. The spectrum of epilepsy and electroencephalographic abnormalities due to SHANK3 loss-of-function mutations. Epilepsia 57, 1651–1659.

Ito-Ishida, A., Ure, K., Chen, H., Swann, J.W., Zoghbi, H.Y., 2015. Loss of MeCP2 in parvalbumin-and somatostatin-expressing neurons in mice leads to distinct rett syndrome-like phenotypes. Neuron 88, 651–658.

Jeste, S.S., Tuchman, R., 2015. Autism spectrum disorder and epilepsy: two sides of the same coin? J. Child Neurol. 30, 1963–1971.

Kajitani, K., Yamaguchi, H., Dan, Y., Furuichi, M., Kang, D., Nakabeppu, Y., 2006. MTH1, an oxidized purine nucleoside triphosphatase, suppresses the accumulation of oxidative damage of nucleic acids in the hippocampal microglia during kainate-induced excitotoxicity. J. Neurosci. 26, 1688–1698.

Lauber, E., Filice, F., Schwaller, B., 2018. Dysregulation of parvalbumin expression in the Cntnap2-/- mouse model of autism spectrum disorder. Front. Mol. Neurosci. 11, 262.

Lee, B.H., Smith, T., Paciorkowski, A.R., 2015. Autism spectrum disorder and epilepsy: disorders with a shared biology. Epilepsy Behav. 47, 191–201.

Lee, S., Lee, E., Kim, R., Kim, J., Lee, S., Park, H., Yang, E., Kim, H., Kim, E., 2018. Shank2 deletion in parvalbumin neurons leads to moderate hyperactivity, enhanced self-grooming and suppressed seizure susceptibility in mice. Front. Mol. Neurosci. 11, 209.

Leitch, B., 2022. The impact of glutamatergic synapse dysfunction in the corticothalamocortical network on absence seizure generation. Front. Mol. Neurosci. 15, 836255.

Lilja, J., Zacharchenko, T., Georgiadou, M., Jacquemet, G., De Franceschi, N., Peuhu, E., Hamidi, H., Pouwels, J., Martens, V., Nia, F.H., Beifuss, M., Boeckers, T., Kreienkamp, H.J., Barsukov, I.L., Ivaska, J., 2017. SHANK proteins limit integrin activation by directly interacting with Rap1 and R-Ras. Nat. Cell Biol. 19, 292–305.

Liu, X., Sun, X., Sun, C., Zou, M., Chen, Y., Huang, J., Wu, L., Chen, W.X., 2021. Prevalence of epilepsy in autism spectrum disorders: a systematic review and meta-analysis. Autism, 13623613211045029.
Makinson, C.D., Tanaka, B.S., Sorokin, J.M., Wong, J.C., Christian, C.A., Goldin, A.L., Escayg, A., Huguenard, J.R., 2017. Regulation of thalamic and cortical network synchrony by Scn8a. Neuron 93 (1165–1179), e1166.
Mao, W., Watanabe, T., Cho, S., Frost, J.L., Truong, T., Zhao, X., Futai, K., 2015. Shank1 regulates excitatory synaptic transmission in mouse hippocampal parvalbumin-expressing inhibitory interneurons. Eur. J. Neurosci. 41, 1025–1035.
Matsushita, Y., Sakai, Y., Shimmura, M., Shigeto, H., Nishio, M., Akamine, S., Sanefuji, M., Ishizaki, Y., Torisu, H., Nakabeppu, Y., Suzuki, A., Takada, H., Hara, T., 2016. Hyperactive mTOR signals in the proopiomelanocortin-expressing hippocampal neurons cause age-dependent epilepsy and premature death in mice. Sci. Rep. 6, 22991.
Maunakea, A.K., Nagarajan, R.P., Bilenky, M., Ballinger, T.J., D'Souza, C., Fouse, S.D., Johnson, B.E., Hong, C., Nielsen, C., Zhao, Y., Turecki, G., Delaney, A., Varhol, R., Thiessen, N., Shchors, K., Heine, V.M., Rowitch, D.H., Xing, X., Fiore, C., Schillebeeckx, M., Jones, S.J., Haussler, D., Marra, M.A., Hirst, M., Wang, T., Costello, J.F., 2010. Conserved role of intragenic DNA methylation in regulating alternative promoters. Nature 466, 253–257.
Monteiro, P., Feng, G., 2017. SHANK proteins: roles at the synapse and in autism spectrum disorder. Nat. Rev. Neurosci. 18, 147–157.
Naisbitt, S., Kim, E., Tu, J.C., Xiao, B., Sala, C., Valtschanoff, J., Weinberg, R.J., Worley, P.F., Sheng, M., 1999. Shank, a novel family of postsynaptic density proteins that binds to the NMDA receptor/PSD-95/GKAP complex and cortactin. Neuron 23, 569–582.
Panthi, S., Leitch, B., 2019. The impact of silencing feed-forward parvalbumin-expressing inhibitory interneurons in the cortico-thalamocortical network on seizure generation and behaviour. Neurobiol. Dis. 132, 104610.
Peca, J., Feliciano, C., Ting, J.T., Wang, W., Wells, M.F., Venkatraman, T.N., Lascola, C. D., Fu, Z., Feng, G., 2011. Shank3 mutant mice display autistic-like behaviours and striatal dysfunction. Nature 472, 437–442.
Penagarikano, O., Abrahams, B.S., Herman, E.I., Winden, K.D., Gdalyahu, A., Dong, H., Sonnenblick, L.I., Gruver, R., Almajano, J., Bragin, A., Golshani, P., Trachtenberg, J. T., Peles, E., Geschwind, D.H., 2011. Absence of CNTNAP2 leads to epilepsy, neuronal migration abnormalities, and core autism-related deficits. Cell 147, 235–246.
Ruden, J.B., Dugan, L.L., Konradi, C., 2021. Parvalbumin interneuron vulnerability and brain disorders. Neuropsychopharmacology 46, 279–287.
Sakai, Y., Okuzono, S., Schaaf, C.P., Ohga, S., 2022. Translational pediatrics: clinical perspective for Phelan-McDermid syndrome and autism research. Pedia Res. 92, 373–377.
Salomaa, S.I., Miihkinen, M., Kremneva, E., Paatero, I., Lilja, J., Jacquemet, G., Vuorio, J., Antenucci, L., Kogan, K., Hassani Nia, F., Hollos, P., Isomursu, A., Vattulainen, I., Coffey, E.T., Kreienkamp, H.J., Lappalainen, P., Ivaska, J., 2021. SHANK3 conformation regulates direct actin binding and crosstalk with Rap1 signaling. Curr. Biol. 31 (4956–4970), e4959.
Sasayama, D., Kuge, R., Toibana, Y., Honda, H., 2021. Trends in autism spectrum disorder diagnoses in Japan, 2009 to 2019. JAMA Netw. Open 4, e219234.
Schmeisser, M.J., Grabrucker, A.M., Bockmann, J., Boeckers, T.M., 2009. Synaptic cross-talk between N-methyl-D-aspartate receptors and LAPSER1-beta-catenin at excitatory synapses. J. Biol. Chem. 284, 29146–29157.
Selimbeyoglu, A., Kim, C.K., Inoue, M., Lee, S.Y., Hong, A.S.O., Kauvar, I., Ramakrishnan, C., Fenno, L.E., Davidson, T.J., Wright, M., Deisseroth, K., 2017. Modulation of prefrontal cortex excitation/inhibition balance rescues social behavior in CNTNAP2-deficient mice. Sci. Transl. Med. 9.
Sharma, V., Sood, R., Lou, D., Hung, T.Y., Levesque, M., Han, Y., Levett, J.Y., Wang, P., Murthy, S., Tansley, S., Wang, S., Siddiqui, N., Tahmasebi, S., Rosenblum, K., Avoli, M., Lacaille, J.C., Sonenberg, N., Khoutorsky, A., 2021. 4E-BP2-dependent translation in parvalbumin neurons controls epileptic seizure threshold. Proc. Natl. Acad. Sci. USA 118.
Wang, X., Xu, Q., Bey, A.L., Lee, Y., Jiang, Y.H., 2014. Transcriptional and functional complexity of Shank3 provides a molecular framework to understand the phenotypic heterogeneity of SHANK3 causing autism and Shank3 mutant mice. Mol. Autism 5, 30.
Warren, A.E.L., Abbott, D.F., Jackson, G.D., Archer, J.S., 2017. Thalamocortical functional connectivity in Lennox-Gastaut syndrome is abnormally enhanced in executive-control and default-mode networks. Epilepsia 58, 2085–2097.
Yang, D.D., Kuan, C.Y., Whitmarsh, A.J., Rincon, M., Zheng, T.S., Davis, R.J., Rakic, P., Flavell, R.A., 1997. Absence of excitotoxicity-induced apoptosis in the hippocampus of mice lacking the Jnk3 gene. Nature 389, 865–870.
Zhu, L., Wang, X., Li, X.L., Towers, A., Cao, X., Wang, P., Bowman, R., Yang, H., Goldstein, J., Li, Y.J., Jiang, Y.H., 2014. Epigenetic dysregulation of SHANK3 in brain tissues from individuals with autism spectrum disorders. Hum. Mol. Genet. 23, 1563–1578.